Springer

Journal of Mechanical Science and Technology 22 (2008) 2318~2327

Journal of Mechanical Science and Technology

www.springerlink.com/content/1738-494x
DOI 10.1007/s12206-008-0720-2

Elastic-plastic thermal stress analysis of an aluminum composite disc under parabolic thermal load distribution †

Gürkan Altan*, Muzaffer Topçu, Numan Behlül Bektaş and Burçin Deda Altan

Department of Mechanical Engineering, Faculty of Engineering, Pamukkale University, Kınıklı 20070 Denizli, Turkey

(Manuscript Received January 9, 2008; Revised June 27, 2008; Accepted July 22, 2008)

Abstract

An elastic-plastic thermal stress analysis was carried out on an orthotropic aluminum metal matrix composite disc with a hole by using an analytical solution. The thermal load distribution was chosen to vary parabolically from inner surface to outer surface. An aluminum composite disc reinforced curvilinearly by steel fibers was produced under hydraulic press. The mechanical properties of the composite disc were obtained from experiments by using strain gauges. A computer program was developed to calculate the thermal stresses under a parabolic temperature from inner surface to outer surface. The material was assumed to be non-linear hardening. The elastic-plastic solution was performed for the plastic region expanded around the inner surface by an analytical method. The magnitude of the tangential stress component for elastic and elastic-plastic was higher than the magnitude of the radial stress component. Besides, the tangential stress component was compressive on the inner surface and tensile on the outer surface. The magnitude of the tangential residual stress component was the highest on the inner surface of the composite disc. The plastic region began at the inner surface of disc.

Keywords: Aluminum composite disc; Thermal stress; Parabolic temperature

1. Introduction

Aluminum composite discs are more commonly preferred in engineering applications such as fly wheels, shrink fits and turbines. In recent times, the proportion of the specific strength to weight has been expected to be higher. Load-carrying capacities of reinforced discs are higher than those of isotropic steel discs with the same geometry. Furthermore, the reinforced discs weigh less than the others. As a result, aluminum composite discs are gaining in popularity.

Analytic solutions for the stress analysis in curvilinearly orthotropic discs and cylinders under different conditions can be found in many books [1-3]. Stanley and Garroch [4] developed a new test method for the composite discs reinforced by molded fiber and obtained thermoelastic data from fiber-reinforced orthotropic disc in this study to find the values of the orientation tensor. Karakuzu and Sayman [5] used the finite-element method and made an elasto-plastic stress analysis in the orthotropic rotating discs with holes. In this study, a nine-node isoparametric rectangular element was selected and Lagrange function was used as interpolation function. They changed the hole radius and loading states at different orientation angles and thus obtained the plastic region distributions and inner stresses on the disc. You and Zhang [6] defined with a polynomial function the relationship between stress and strain for the discs made from hardening material. They derived from the von Mises yield criterion the primary equation of the discs under plane stress, fixed thickness and fixed density, and they described the relationship between stress and strain. Stanley and Singh and Ray [7] determined the creep on an orthotropic aluminum silicon carbide composite rotating disc according to the Tsai-Hill

† This paper was recommended for publication in revised form by Associate Editor Joo Ho Choi

*Corresponding author. Tel.: +90 258 296 3163, Fax.: +90 258 296 3262
E-mail address: gurkanaltan@pau.edu.tr

yield criterion. The results obtained from this study were compared with the ones from the von Mises yield criterion used for isotropic composites. Sayman [8] used an analytical method to investigate thermoelastic stress analysis on an orthotropic composite disc with aluminum metal matrix. Çallıoğlu et al. [9] studied stress analysis analytically on a circular orthotropic rotating disc under mechanic and thermal load. They obtained the solutions under parabolic temperatures along a radial section from the inner surface of the disc to the outer surface. They compared these results with the results of another Çallıoğlu's [10] study. In this study, he studied a stress analysis on a rotating hallow disc made of rectilinear glass-fiber epoxy prepreg under thermal loading that is varying parabolically from inner surface to outer surface along the radial section. Garroch and Stanley [11] applied the test method that they developed to a composite disc. They obtained thermo elastic data from the center of a fiber-reinforced orthotropic disc under pressure along its diameter for a disc orientation. Bektaş et al. [12] applied the elastic-plastic stress analysis on a curvilinear steel fiber reinforced aluminum composite disc with an aluminum metal matrix under internal pressure loads. To obtain the plastic stresses, they used an analytical method that Bektaş and Sayman had already developed in their earlier studies [13]. Sayer et al. [14] manufactured a low density thermoplastic composite disc reinforced with E-glass fibers and obtained thermo-elastic stresses under uniform and linear temperature distribution.

In the present work, aluminum composite discs reinforced by steel fibers were produced and their mechanical properties were calculated through experiments. Elastic-plastic stress analysis of the composite disc under parabolic temperature distribution was made analytically by using the Fortran computer program. The detailed results of this study and information are given by Altan [15]. A summary of that information is presented in this study along with the results. Elastic, elastic-plastic and residual thermal stress distributions were obtained analytically from inner surface to outer surface along the radial section and they were presented in tables and figures.

2. Production of the aluminum composite disc

Aluminum matrix was reinforced by the steel fibers of a circular form [15]. The composite disc was manufactured in two steps. In the preparation stage, moulds and materials to make up the disc were prepared. As seen in Fig. 1, a mould was prepared with an internal diameter of 160 mm. As the material of matrix, aluminum plates of a circular form were used. As the fiber material, steel wire was used. Circular form was given to the steel wire in such a way as to create circles ranging from 40 mm to 155 mm in diameter. As seen in Fig. 1, steel fibers of a circular form were placed on the aluminum plates and brought to the stage of composite disc manufacture.

Composite disc manufacture was carried out under pressure by means of a hydraulic press. The plates into which resistance was placed to heat the materials that would make up the aluminium composite disc were mounted on the lower and upper platform of the press. Pressure was applied to the aluminum plates and steel fibers heated by the plates with lower and upper resistance. The moulds were heated up to 550 °C with the use of electrical resistances in the course of manufacture and 30 MPa pressure was applied with the press on them for 10 minutes. Under these circumstances, aluminum plates were amalgamated and made up the matrix of the manufactured composite disc. The steel wires within the aluminum matrix made up the fibers of the manufactured composite disc.

3. Mechanical properties of composite material

Mechanical properties of the composite material were obtained by strain gauges and Instron test machine. Elasticity modulus perpendicular to fibers, namely radial elasticity modulus, was defined as (E_r) . As seen in Fig. 2, two strain gauges were placed in the direction of the loading axis, namely, in the radial direction, and in a perpendicular direction to loading axis, namely, in the tangential direction. Radial elas-

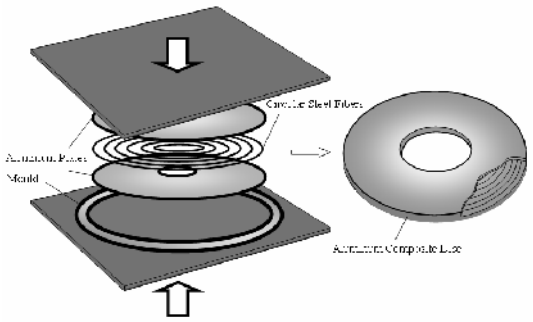

Fig. 1. A schematic view of composite disc manufacturing [15].

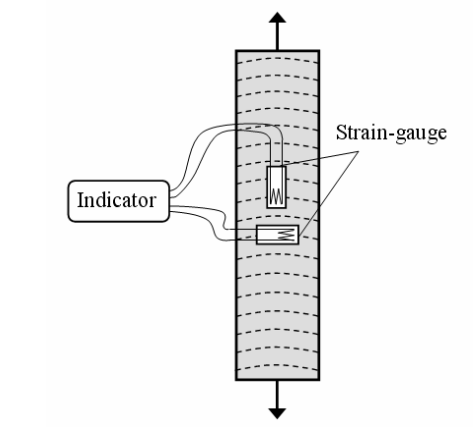

Fig. 2. Specimen of radial elasticity.

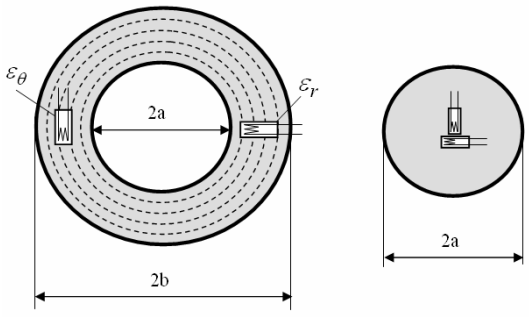

Fig. 3. (a) Composite disc, (b) Aluminum disc.

ticity modulus (E_r) and Poisson's ratio $\nu_{r\theta}$ were determined from the average deformations both in radial direction and tangential direction.

Elasticity modulus in the direction of material's reinforcement was defined as the tangential elasticity modulus (E_θ). To determine the tangential elasticity modulus, a circular aluminum disc on which strain-gauges were placed as seen in Fig. 3 was placed in the composite disc. After the process of placing, some contraction was observed in the aluminum disc. Stress components that occurred on the aluminum disc because of the external pressure are shown in Eq. (1) [2].

$$\sigma_r = \sigma_\theta = -p \tag{1}$$

External pressure on the aluminum disc was found as p= -2.5 MPa with a view to the equation of radial and tangential stress.

Distribution of stress in a hollow disc exposed to uniform pressure on internal and external surfaces is shown in Fig. 4. The p and q stand for the values of

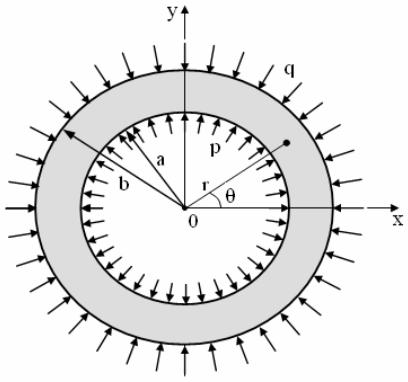

Fig. 4. Composite disc exposed to uniform internal and external pressures.

uniform internal and external pressures, while a and b represent the internal and external radius of the disc. The stresses consequent upon it are given below by using Ref [1].

External pressure that occurs on the aluminum disc affects the composite disc from the inner surface of it as the internal p pressure with a uniform distribution. As no external pressure affects the composite disc, q=0 is accepted. The radial and tangential stresses that occur in this case are calculated with the use of (k) in Eqs. (4)-(5).

$$\sigma_r = \frac{p\, c^{k+1}}{1-c^{2k}} \frac{\rho^{2k}-1}{\rho^{k+1}} \tag{2}$$

$$\sigma_\theta = \frac{p\, k\, c^{k+1}}{1-c^{2k}} \frac{\rho^{2k}+1}{\rho^{k+1}} \tag{3}$$

where

$$c = \frac{a}{b},\ \rho = \frac{r}{b}\ \ (c\langle 1,\ c \le \rho \le 1),\ k^2 = \frac{E_\theta}{E_r} = \frac{\nu_{\theta r}}{\nu_{r\theta}}$$

Radial and tangential stresses may also be found by the strains measured over the composite disc. Stress-strain correlation for orthotropic materials by using the Ref [16] can be obtained in the following way:

$$\sigma_r = E_r \frac{\varepsilon_r + \nu_{r\theta} k^2 \varepsilon_\theta}{1-\nu_{r\theta}^2 k^2} \tag{4}$$

$$\sigma_\theta = E_r k^2 \frac{\varepsilon_r \nu_{r\theta} + \varepsilon_\theta}{1-\nu_{r\theta}^2 k^2} \tag{5}$$

The value of (k) was found as 1.12 by equalization of these two tangential stress components (Eq. (3) and

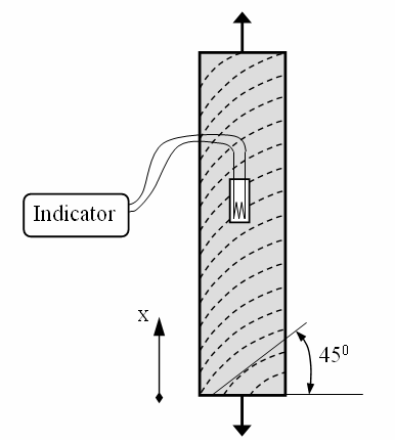

Fig. 5. Shear specimen.

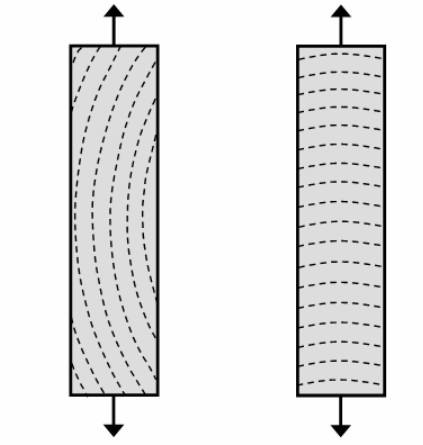

Fig. 6. Specimens for (a) X and (b) Y yield strengths.

Eq. (5)). As a result of this, E_θ and $\nu_{\theta r}$ were found as 89500 MPa and 0.28, respectively.

As seen in Fig. 5, fiber directions of the shear specimen have a 45° angle. Shear modulus ($G_{\theta r}$) was determined approximately by the test specimen [17].

Yield strength of the composite material in the direction of fiber was shown with (X), and the yield strength of the composite material (Y) that occurred on an axis perpendicular to fiber direction. In Fig. 6, the specimens in the direction of fiber and perpendicular to fiber direction are shown. (X) and (Y) yield strengths were found as 97 MPa and 36 MPa, respectively, by means of the Instron testing machine.

Shear yield strength (S) was measured by the Iosipescu test method. The loading apparatus used in the Iosipescu test method is shown in Fig. 7. By means of the Iosipescu loading apparatus, a pure shear load with no contortion takes place between the notches of the specimen. Shear yield strength is calculated by using the maximum shear load that takes place on the loading apparatus.

Table 1. Mechanical properties of aluminum composite disc.

E_θ (MPa)	E_r (MPa)	$G_{\theta r}$ (MPa)	$\nu_{\theta r}$	X (MPa)	Y (MPa)	S (MPa)	K (MPa)	n	α_θ (1/°C)	α_r (1/°C)
89500	71500	32000	0.28	97	36	48	157.6	0.47	$18.6.10^{-6}$	$21.6.10^{-6}$

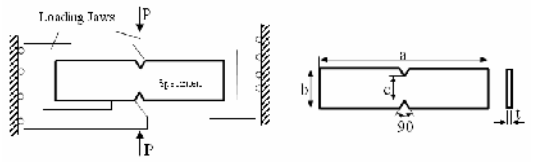

Fig. 7. Iosipescu loading apparatus.

$$S = \frac{P_{\max}}{t.c} \tag{6}$$

Thermal expansion coefficients were found by using micro mechanic models and considering the property of the material [17]. Mechanic properties of the composite disc manufactured are given in Table 1.

4. Elastic solution

The strain-stress correlation that takes place on an orthotropic composite disc under the influence of temperature can be written as follows:

$$\varepsilon_r = a_{rr}\,\sigma_r + a_{r\theta}\,\sigma_\theta + \alpha_r T \tag{7}$$

$$\varepsilon_\theta = a_{r\theta}\,\sigma_r + a_{\theta\theta}\,\sigma_\theta + \alpha_\theta T \tag{8}$$

Here α_r and α_θ are thermal expansion coefficients in the radial and tangential directions. Constants of the a_{rr}, $a_{r\theta}$ and $a_{\theta\theta}$ elasticity matrix are as follows:

$$a_{\theta\theta} = \frac{1}{E_\theta},\ a_{rr} = \frac{1}{E_r} \quad \text{and} \quad a_{r\theta} = a_{\theta r} = -\frac{\nu_{r\theta}}{E_r} = -\frac{\nu_{\theta r}}{E_\theta}$$

If the stress distribution is, as seen in Fig. 4, symmetrical to an axis that passes from 0 and that is perpendicular to x-y plane, stress components cannot be dependent on 'θ' and become the functions of 'r' only. Because of the symmetry, the value of $\tau_{r\theta}$ shear stress is equal to zero. The equilibrium equation for the plane stress case can be written as follows:

$$r\frac{d\sigma_r}{dr}+\sigma_r-\sigma_\theta=0 \tag{9}$$

Stress components as in Eq. (10), obtained from an F stress function, secure the equilibrium equation in Eq. (9).

$$\sigma_r=\frac{F}{r} \quad \text{and} \quad \sigma_\theta=\frac{dF}{dr} \tag{10}$$

$$\varepsilon_r=\frac{du}{dr} \quad \text{and} \quad \varepsilon_\theta=\frac{u}{r} \tag{11}$$

and the relation between strains can be written as follows:

$$\varepsilon_r=\frac{d}{dr}(r.\varepsilon_\theta) \tag{12}$$

Accordingly, Eqs. (7)-(9) can be written as follows:

$$\frac{du}{dr}=a_{rr}\frac{F}{r}+a_{r\theta}\frac{dF}{dr}+\alpha_r T \tag{13}$$

$$\frac{u}{r}=a_{r\theta}\frac{F}{r}+a_{\theta\theta}\frac{dF}{dr}+\alpha_\theta T \tag{14}$$

If these equations are put in their place in the compatibility equation Eq. (12), the differential equation of the F stress function is found as follows.

Considering $k^2=\frac{a_{rr}}{a_{\theta\theta}}=\frac{E_\theta}{E_r}$;

$$r^2F''+rF'-k^2F=\frac{(\alpha_r-\alpha_\theta)\,T}{a_{\theta\theta}}r-\frac{\alpha_\theta T'}{a_{\theta\theta}}r^2 \tag{15}$$

As seen in Fig. 8, to find the distribution of the stresses when $T=T_0$ in the internal surface and under temperature distribution parabolic towards the outer surface where T=0 °C, the differential equality in Eq. (15) is denoted for the F stress function. The stress function F can be obtained by using the transform of $r=e^t$.

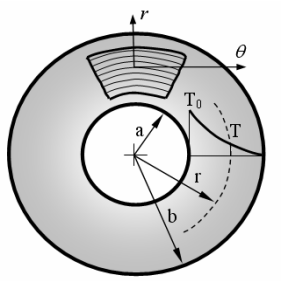

Fig. 8. Aluminium composite disc under parabolic temperature distribution.

The relationship between parabolic temperature and equation, and F stress function are as follows:

$$T=T_0\frac{b^2-r^2}{b^2-a^2} \tag{16}$$

$$F=C_1r^k+C_2r^{-k}+Kr^3+Mr \tag{17}$$

Here C_1 and C_2 are arbitrary integral constants and K and M constants are as follows:

$$K=\frac{(3\alpha_\theta-\alpha_r)}{a_{\theta\theta}(b^2-a^2)(9-k^2)}T_0$$

$$\text{and} \quad M=\frac{b^2(\alpha_r-\alpha_\theta)}{a_{\theta\theta}(b^2-a^2)(1-k^2)}T_0 \tag{18}$$

σ_r and σ_θ stress components can be found from F stress function as follows:

$$\sigma_r=C_1r^{k-1}+C_2r^{-k-1}+M+Kr^2 \tag{19}$$

$$\sigma_\theta=C_1kr^{k-1}-C_2kr^{-k-1}+M+3Kr^2 \tag{20}$$

C_1 and C_2 arbitrary integral constants can be found with the use of limit conditions mentioned below:

$\sigma_r=0$ at the r = a , $\sigma_r=0$ at the r = b

$$C_1=M\frac{(a^{k+1}-b^{k+1})}{b^{2k}-a^{2k}}+K\frac{(a^{k+3}-b^{k+3})}{b^{2k}-a^{2k}} \tag{21}$$

$$C_2=M\frac{a^{2k}b^{k+1}-b^{2k}a^{k+1}}{b^{2k}-a^{2k}}+K\frac{(a^{2k}b^{k+3}-a^{k+3}b^{2k})}{b^{2k}-a^{2k}} \tag{22}$$

Tangential and radial stress components under the load of parabolic temperature can be found in this way.

5. Plastic solution

Diffusion of the plastic deformation is found as a yield criterion. The Tsai-Hill criterion is used in elastic-plastic stress analysis of the composite materials [16]. Equivalent stress in the direction of fiber according to Tsai-Hill criterion is as follows:

$$\sigma_{eq}=\sqrt{\sigma_\theta^2-\sigma_r\sigma_\theta+\frac{\sigma_r^2X^2}{Y^2}} \tag{23}$$

If the equivalent stress is bigger than the yield stress, elasto-plastic stress occurs. Here X and Y

stresses indicate the yield stresses in tangential and radial directions. Stress value in the non-linear hardening plastic region is given below according to Ludwik equation:

$$\sigma = \sigma_0 + K\varepsilon_p^n \tag{24}$$

Here K is the plasticity constant and n is the hardening exponential. σ_0 yield stress is equal to X. The strain increments are as follows [18].

$$\begin{aligned} d\varepsilon_r &= a_{rr}d\sigma_r + a_{r\theta}d\sigma_\theta + d\varepsilon_r^p + \alpha_r dT \\ d\varepsilon_\theta &= a_{r\theta}d\sigma_r + a_{\theta\theta}d\sigma_\theta + d\varepsilon_\theta^p + \alpha_\theta dT \end{aligned} \tag{25}$$

Plastic strain increments were determined from plastic potential energy according to Prandtl-Reuss equation for anisotropic materials [3]. Accordingly, plastic potential energy is a scalar function of stress.

$$f_{ij} = \sigma_{eq} \tag{26}$$

and plastic strain increments occur according to the flow rule.

$$d\varepsilon_{ij}^p = \frac{\partial f_{ij}}{\partial \sigma_{ij}} d\lambda \tag{27}$$

$d\lambda$ is a constant that is equal to equivalent plastic strain $d\varepsilon_p$ value. The tangential stress component is obtained as follows from the equivalent equation.

$$\sigma_\theta = \sigma_r + r\frac{d\sigma_r}{dr} \tag{28}$$

If the σ_θ tangential stress component, which is obtained from equivalent equation, is put in its place in the Tsai-Hill yield criterion, $d\sigma_r$ is found as follows.

$$r^2\left(\frac{d\sigma_r}{dr}\right)^2 + r\sigma_r\frac{d\sigma_r}{dr} + \sigma_r^2\frac{X^2}{Y^2} = {\sigma_{eq}}^2 \tag{29}$$

$$d\sigma_r = \frac{-r\sigma_r \pm \sqrt{r^2\sigma_r^2 - 4r^2\left(\frac{X^2}{Y^2}\sigma_r^2 - {\sigma_{eq}}^2\right)}}{2r^2}dr \tag{30}$$

Plastic strain increments are obtained as follows.

$$\begin{aligned} d\varepsilon_r^p &= \frac{\partial f}{\partial \sigma_r}d\lambda = \frac{-\sigma_r + 2\sigma_r X^2/Y^2}{2\bar{\sigma}}d\varepsilon_p \\ d\varepsilon_\theta^p &= \frac{\partial f}{\partial \sigma_\theta}d\lambda = \frac{2\sigma_\theta - \sigma_r}{2\bar{\sigma}}d\varepsilon_p \end{aligned} \tag{31}$$

The relationship between ε_r^p and ε_θ^p is obtained as follows.

$$\begin{aligned} &dr[\sigma_r(a_{rr} - a_{r\theta}) + \sigma_\theta(a_{r\theta} - a_{\theta\theta}) + \varepsilon_r^p - \varepsilon_\theta^p + T(\alpha_r - \alpha_\theta)] \\ &-a_{r\theta}rd\sigma_r - a_{\theta\theta}rd\sigma_\theta - rd\varepsilon_\theta^p - \alpha_\theta rdT = 0 \end{aligned} \tag{32}$$

Here: $\varepsilon_r^p = \sum d\varepsilon_r^p$ and $\varepsilon_\theta^p = \sum d\varepsilon_\theta^p$

Tsai-Hill yield criterion:

$$\begin{aligned} &2\sigma_\theta d\sigma_\theta - \sigma_\theta d\sigma_r - \sigma_r d\sigma_\theta + 2\sigma_r\frac{X^2}{Y^2}d\sigma_r \\ &= 2\bar{\sigma}Kn\varepsilon_p^{n-1}d\varepsilon_p \end{aligned} \tag{33}$$

σ_r and σ_θ stress components are found from Eq. (28) and Eq. (30). Plastic strain increments are obtained from Eqs. (31)- (33).

The plastic region expands from the internal radius of the disc to its external radius. As seen in Fig. 9, between the radius a and radius c is the plastic region and between the radius c and radius b is the elastic region.

The stresses that occur on the radius c, which makes the elastic and plastic boundary, are found by using the elastic radial stress component. The radial stress component on the elastic boundary is equal to the radial stress component on the plastic boundary.

$$\sigma_r = C_1 r^{k-1} + C_2 r^{-k-1} + M + Kr^2 \tag{34}$$

Since the radial stress component is equal to the p stress at the elastic-plastic boundary, then boundary conditions are as follows.

$$\sigma_r = p \quad \text{at} \quad r = c$$
$$\sigma_r = 0 \quad \text{at} \quad r = b$$

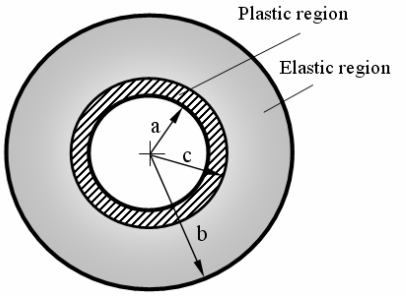

Fig. 9. Distribution of elastic and plastic regions in the composite disc.

Using these boundary conditions, we can find the C_1 and C_2 coefficients as follows.

$$C_1 = M\frac{(c^{k+1}-b^{k+1})}{b^{2k}-c^{2k}} + K\frac{(c^{k+3}-b^{k+3})}{b^{2k}-c^{2k}} - \frac{pc^{k+1}}{b^{2k}-c^{2k}} \tag{35}$$

$$C_2 = M\frac{c^{2k}b^{k+1}-b^{2k}c^{k+1}}{b^{2k}-c^{2k}} + K\frac{(c^{2k}b^{k+3}-c^{k+3}b^{2k})}{b^{2k}-c^{2k}} + \frac{pc^{k+1}b^{2k}}{b^{2k}-c^{2k}} \tag{36}$$

Using the arbitrary integral constants in Eqs (35)-(36), we can find the stress components in the elastic region after the radius c, namely, elastic and plastic boundary.

6. Results and discussion

In the present study, an analytical method was used to determine the elastic-plastic thermal stresses under the parabolic temperature distribution for non-linear hardening material behavior. The solution of the analytical method was made by means of the Fortran computer program. During the solution, it was assumed that thermal stresses are zero at 0°C and the material properties do not depend on the temperature variations. According to these assumptions, radial and tangential stress components were found in a variety of temperature distributions such as ΔT_0=94.6, 100, 105 and 110°C, from the inner surface of the disc to its outer surface. Composite material is accepted as a non-linear hardening one in the plastic region, and elasto-plastic solution of the composite disc is obtained analytically. The beginning of plastic yield was determined according to Tsai-Hill yield criterion. It was also determined how the plastic region expanded from the inner surface of the disc to its outer surface. The residual stresses were obtained from the superimposition of plastic and elastic stresses.

Thermal elastic-plastic stress analysis results under the parabolic temperature distribution are given in Table 2. The magnitude of the equivalent stress is the highest on the inner surface. As a result, the plastic yielding occurs first on the inner surface at 94.6°C. So, plastic yielding starts at ΔT_0=94.6°C from the inner surface of the disc to its outer surface. As seen in Table 2, diffusion of the plastic region increases with the rise in temperature. It is seen from the table and figures that elastic and plastic radial stress compo-

Table 2. Stress components at the inner and outer disc surfaces under parabolic temperature distribution.

Temperature ΔT_0 (°C)	Plastic boundary r (mm)	Surfaces	ε_p	Elastic stresses (MPa)		Plastic stresses (MPa)		Residual stresses (MPa)	
				$(\sigma_r)_e$	$(\sigma_\theta)_e$	$(\sigma_r)_p$	$(\sigma_\theta)_p$	$(\sigma_r)_r$	$(\sigma_\theta)_r$
94.6	15.0	Inner	0.000	0.00	-97.00	0.00	-97.00	0.00	0.00
		Outer	0.000	0.00	82	0.00	82	0.00	0.00
100	15.4	Inner	0.060	0.00	-102.59	0.00	-97.00	0.00	5.59
		Outer	0.000	0.00	86.68	0.00	86.87	0.00	0.19
105	15.8	Inner	0.250	0.00	-107.72	0.00	-97.00	0.00	10.72
		Outer	0.000	0.00	91.02	0.00	91.41	0.00	0.39
110	16.4	Inner	0.570	0.00	-112.84	0.00	-97.00	0.00	15.84
		Outer	0.000	0.00	95.35	0.00	96.08	0.00	0.73

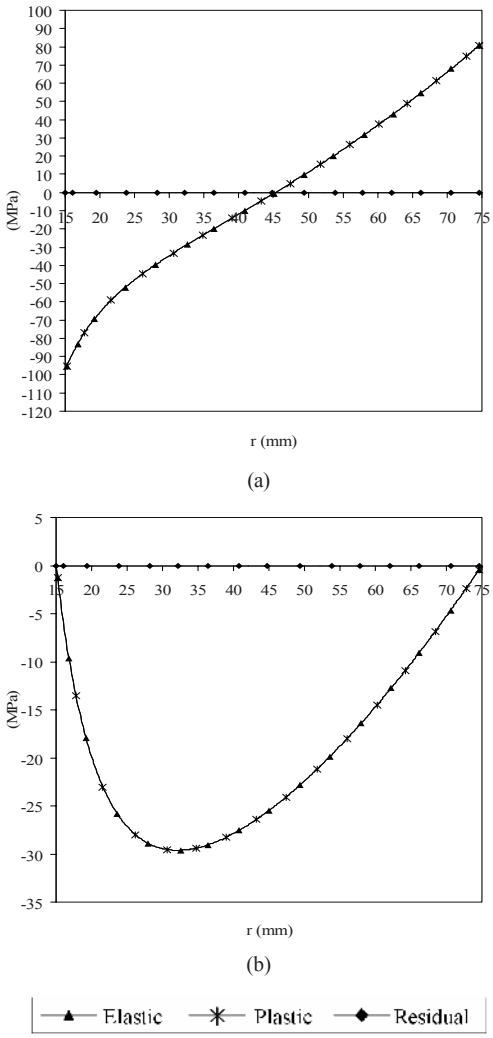

Fig. 10. Tangential stress components (a), radial stress components (b) and residual stress components for ΔT_0=94.6°C.

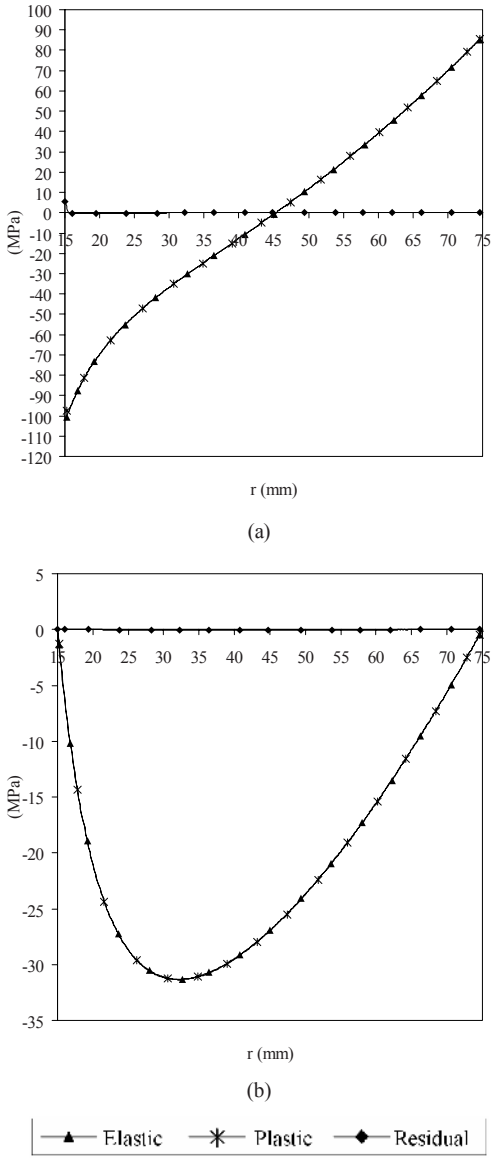

Fig. 11. Tangential stress components (a), radial stress components (b) and residual stress components for ΔT_0=100°C.

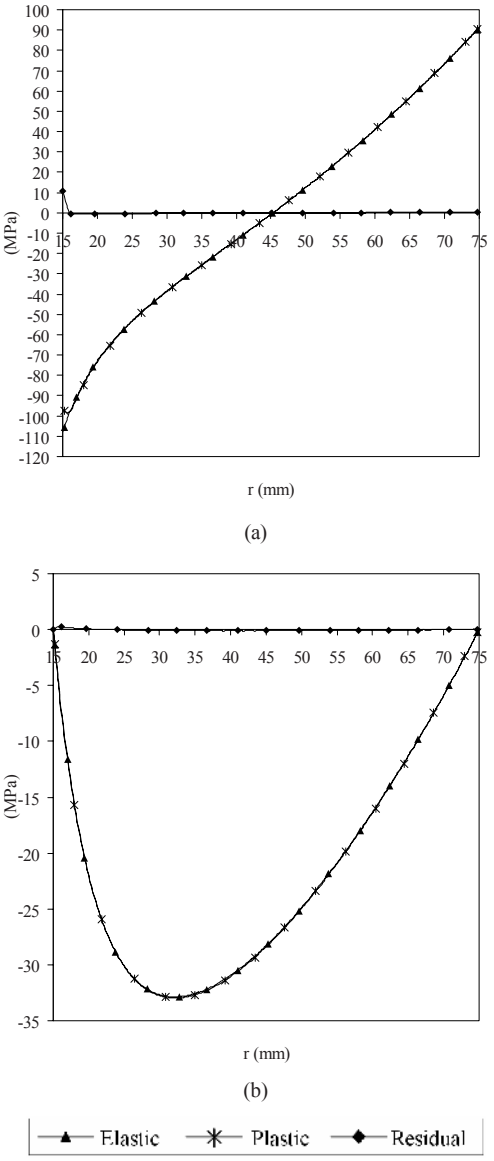

Fig. 12. Tangential stress components (a), radial stress components (b) and residual stress components for ΔT_0=105°C.

nents are zero in the inner and outer surfaces of the disc. The values of tangential stress components increase with the rise in temperature.

The distributions of tangential and radial stress components along the radial section for elastic and plastic solution at yielding temperature are shown in Fig. 10. Since ΔT_0=94.6°C was found as the boundary of plastic yielding, the values of elastic and plastic stresses are equal, and accordingly the values of the residual stress components are zero. Tangential stress components remain as compressive around the inner surfaces of the disc and as tensile around its outer surfaces. Radial stress components are zero in the inner and outer diameter boundaries and always remain as compressive in between them.

The distributions of the elastic, elastic-plastic and residual stress of the tangential, and radial stress components at ΔT_0=100°C are depicted in Fig. 11. As seen in Fig. 11(a), tangential residual stresses remain as tensile in the inner part of the disc, as compressive

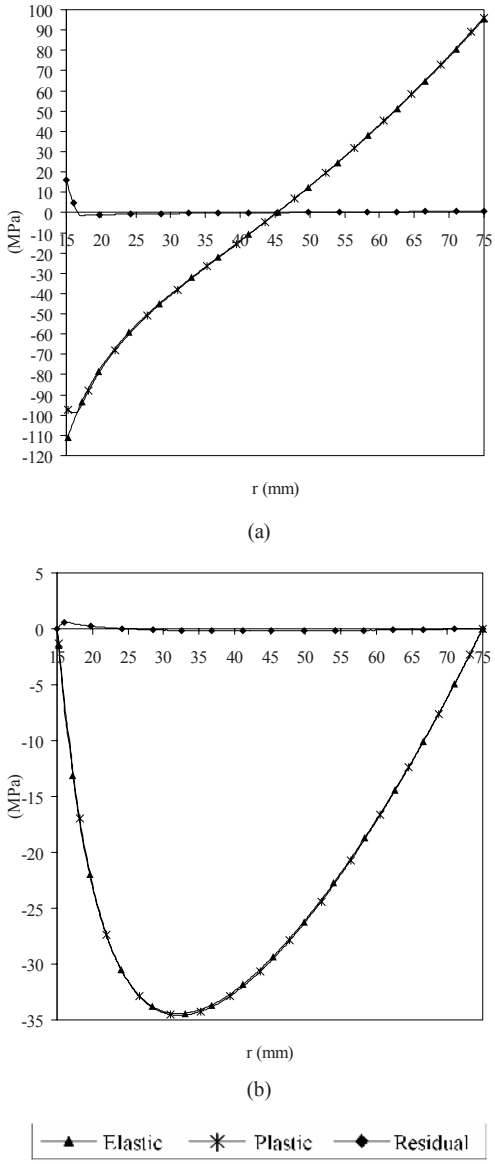

Fig. 13. Tangential stress components (a), radial stress components (b) and residual stress components for ΔT_0=110°C.

in between its plastic boundary and middle part, and as tensile again in its outer part. Tangential residual stresses in the inner surface of the disc are bigger. As seen in Fig. 11(b), radial residual stresses remain as tensile in the inner surface of the disc and as compressive in its parts after its plastic boundary. The values are equal to zero only in the inner and outer surfaces of the disc. For 105 and 110°C temperatures, distributions of tangential and radial elastic, elasto-plastic and residual stress components are given in Figs. 12-13.

7. Conclusions

The following conclusions are obtained from the thermal elastic-plastic stress analysis of a composite disc with aluminum metal-matrix under a load of parabolic temperature.

- The magnitude of the equivalent stress is the highest on the inner surface. As a result, plastic yielding first starts from the inner surface of the composite disc.
- With increasing temperature, the plastic region begins to expand from the inner surface to the outer surface.
- The magnitude of tangential stress components is higher than that of the radial stress components.
- Tangential stress components are compressive in the inner parts of the composite disc but tensile in its outer parts.
- Radial stress components are zero in the inner and outer surfaces of the composite disc and remain as compressive in the middle parts of it.
- Residual stress is obtained from elastic and plastic solutions.

References

[1] S. G. Lekhnitskii, Theory of Elasticity of an Anisotrpic Body, Mir Publishers, Moscow, (1981).

[2] S. P. Timoshenko and J. N. Goodier, Theory of Elasticity, McGraw-Hill Company, Singapore, (1970).

[3] W. Johnson and P. B. Mellor, Engineering Plasticity, Von Nastrand Reinhold Comp., London, (1978).

[4] P. Stanley and C. Garroch, A thermoelastic disc test for the mechanical characterisation of fibre-reinforced moulded composites: Theory, Composites Science and Technology, 59 (1999) 371-378.

[5] R. Karakuzu and O. Sayman, Elasto-plastic finite element analysis of orthotropic rotating discs with holes, Computers & Structures, 51 (6) (1994) 695-703.

[6] L. H. You and J. J. Zhang, Elastic-plastic stresses in a rotating solid disk, International Journal of Mechanical Sciences, 41 (1999) 269-282.

[7] S. B. Singh and S. Ray, Modelling the anisotropy and creep in orthotropic aluminum-slicon carbide composite rotating disc, Mechanics of Materials, 34 (2002) 363-372.

[8] O. Sayman, Thermal stress analysis in an aluminum metal-matrix ortotropic disc, Journal of Reinforced

Plastics and Composites, 23 (2004) 1473-1479.
[9] H. Çallıoğlu, M. Topcu and G. Altan, Stress analysis of curvilinearly orthotropic rotating disc under mechanical and thermal loading, Journal of Reinforced Plastics and Composites, 24 (2005)831-838.
[10] H. Çallıoğlu, Stress Analysis of an orthotropic rotating disc under thermal loading, Journal of Reinforced Plastics and Composites, 23 (2004) 1859-1867.
[11] C. Garroch and P. Stanley, A thermoelastic disc test for the mechanical characterisation of fibre-reinforced moulded composites: Application, Composites Science and Technology, 59 (1999) 379-389.
[12] N. B. Bektaş, M. Topcu, H. Çallıoğlu and G. Altan, Elastic-plastic and residual stress analysis of an aluminum metal-matrix composite disk under internal pressures, Journal of Reinforced Plastics and Composites, 24 (2005) 753-762.
[13] N. B. Bektaş and O. Sayman, Elastic-plastic stress analysis in simply supported thermoplastic laminated plates under thermal loads, Composites Science and Technology, 61 (2001) 1695-1701.
[14] M. Sayer, M. Topcu, N. B. Bektaş and A. R. Tarakcilar, Thermo-elastic stress analysis in a thermoplastic composite disc, Science and Engineering of Composite Materials, 12 (2005) 251-260.
[15] G. Altan, Thermal Stress Analysis of Composite Discs, M.Sc. Thesis, Pamukkale University, Denizli, Turkey, (2004).
[16] R. M. Jones, Mechanics of Composite Materials, McGraw-Hill Company, Kogakusha, Tokyo, (1975).
[17] R. F. Gibson, Principle of Composite Material Mechanics, McGraw-Hill, Singapore, (1994).
[18] J. Chakrabarty, Theory of Plasticity, McGraw-Hill Company, Singapore, (1988).

Gürkan Altan is a Research Assistant of Mechanical Engineering at the University of Pamukkale, Denizli, Turkey. Gürkan Altan received the B.E. degree (1999) in mechanical engineering from Dokuz Eylül University, Izmir, and the M.S. degree (2004) in mechanical engineering from Pamukkale University, Denizli. Gürkan Altan is interested in production and applications of composite materials. Currently he is involved in the development and application of joints of composite structures.